Vol. 47, No. 2 (2025) 342-354, DOI: 10.24874/ti.1851.01.25.04

Tribology in Industry

www.tribology.rs

RESEARCH

Wear Analysis of Manganese Steel in Order to Develop Mathematical Model

Rakesh Kumar[a], Bipin Kumar Singh[b,*], Rahul Sinha[c], Rakesh Kumar[c], Sujeet Kumar Gautam[d], K. Karthik Selva Kumar[e]

[a]*Elitte College of Engineering, Kolkata-700113, West Bengal, India,*
[b]*Centre for Augmented Intelligence and Design, Department of Mechanical Engineering, Sri Eshwar College of Engineering, Coimbatore - 641202, Tamil Nadu, India,*
[c]*School of Engineering, P P Savani University, Surat, 394125, Gujarat, India,*
[d]*Department of Foundry and Forge Technology, National Institute of Advanced Manufacturing Technology, Hatia, Ranchi, 834003, Jharkhand, India,*
[e]*Department of Green Energy Technology, Madanjeet School of Green Energy Technologies, Pondicherry University, Indi.*

Keywords:

Manganese steel
Coal particles
Abrasion
Grain Size
Wear

* Corresponding author:

Bipin Kumar Singh
E-mail: bipinmech2008@gmail.com

Received: 2 January 2025
Revised: 22 February 2025
Accepted: 22 April 2025

A B S T R A C T

Manganese steel, commonly known as Hadfield steel, offers exceptional strength, toughness, corrosion resistance, and durability against heavy impact and abrasion, making it suitable for a wide range of industrial applications. However, the limited research on wear phenomena during operation hinders its broader application. Therefore, this study extensively examines the factors contributing to wear in manganese steel, with a focus on raw coal as abrasive particles. The work begins by selecting two coal particle sizes (500 μm and 710 μm) as abrasives, which are positioned between the disc and the manganese steel pin. The experiments also investigate the effect of load, ranging from 20 to 35 N, on the wear behavior of manganese steel. Additionally, SEM images of all wear tracks are captured at the same magnification to analyze changes in wear patterns. The study found that larger abrasive particles have a more detrimental impact on wear compared to smaller ones. Furthermore, a mathematical model is developed to predict theoretical wear losses based on experimental results. The findings demonstrate that the mathematical model aligns well with the experimental data, supporting its applicability in real-world scenarios.

1. INTRODUCTION

Abrasive wear in mechanical components is well-documented as a cause of production losses and increased maintenance costs. Understanding and managing the abrasives that cause wear can help reduce this effect to some extent. In this context, Jost [1] published a book highlighting that proper attention to abrasive wear could yield a cost-to-benefit ratio of 1:40. Another book published by Davies [2] focused on condition monitoring and the failure

(degradation) of materials during operation, specifically related to manufacturing industries. Researchers concluded that the failure or loss of material during functioning were highly attributed to abrasive wear, approx. 50 %, followed by adhesive wear, erosive wear, fretting wear and corrosive wear also have contributions of 15 %, 8 %, 8 % and 5 % respectively. Furthermore, the documented literature highlighted that the two-body abrasion results in more surface damage due to direct contact between them [3-5]. Further, the wear of the mechanical components creates serious repair, which account for cost and time. Wear-resistant material is provided to protect the main mechanical components of machines from wear. Therefore, manganese steel material, governing excellent work-hardening properties, found many applications in numerous industries particularly in mining industries and coal bunker liner plates [6-7].

For Manganese or austenitic steel, popularly known as Hadfield steel, was first proposed by Robert Hadfield in 1941 and led to a revolutionary era for many industries [8]. After the invention of manganese steel, it has been widely used in mining, steel making, and railroading. Manganese steel stands in a wide range of demanding applications in several industries due to its well-known properties, i.e., resistance against wear, good toughness, high strength, damping, and non-magnetic. Manganese steel proves to be suitable for applications like damping, which provides noise proof in construction, and wear resistance requirements such as liners for crushers, excavator buckets, pipes for slurry transportation in mines, and many more [9]. It is also noticed that the properties like corrosion and abrasion resistance could be enhanced by changing the composition of alloying elements in manganese steel. As the weight percentage of manganese in Hadfield steel is 12 wt.% manganese, it shows high toughness and good wear resistance properties when applied to carry the work against a wear environment [10-11]. Researchers noticed [12] that the wear resistance property, depending on the material hardness, was not enough to examine material wear resistance. Some literature stated that the manganese steel shows an increase in hardness after abrasion [13]. In this regard, Zambrano et al. [14] stated that the increase in hardness during abrasion was dedicated to the theory of dipole interaction and stacking fault energy. The mechanism was earlier revealed by Bayraktar et al. [15], illustrating that the wear-resistant property of manganese steel depends on the dislocation property of C-Mn dipole interaction. In comparison, Song et al. [16] stated that due to the change in strain-induced martensite ($\gamma \rightarrow \varepsilon$ or $\acute{\alpha}$), the manganese steel shows enhance strain hardenability. The creation of strain-induced martensite on manganese steel surface was related to stacking fault energy (SFE). The SFE depends on grain size, chemical composition, and microstructure that provide difficult to move the grains from their original position. The mechanism was attributed to the formation of the Hall-Petch effect as earlier demonstrated by Pierce et al. [17]. In many cases, it has been observed that the movement of surface grain during dislocations results in surface grain refinement, which is a part of the dynamic Hall-Petch effect. Acselrad et al. [18] noted that the increase in SFE of manganese steel decreases its wear. Some investigations also showed that the wear of manganese steel was dependent on the sizes of abrasive particles, the apex angle of the abrasive, and the hardness of the abrasive [19-20]. Rabinowicz and Mutis [21] reported that the wear was more if the size of the abrasive particle was large. Furthermore, the analysis also reported regarding the critical size of particles beyond which wear was independent of the critical size. The contact mechanism between an abrasive particle and metal surface with respect to the diameter of the abrasive particle, the load applied on the abrasive, along with the apparent area of contact was demonstrated by Wang and Hutchings [22]. Based on the results of abrasive wear tests, researchers concluded that the scratches were dependent on the load as well as abrasive particles (different sizes). Moore and Douthwaite [23] reported that the large size of abrasive particles produces grooves of considerable depth. The degree of groove formation on the material surface also increases with the sharpness of the abrasive particles. The apex angle of the abrasive particle was used to measure its sharpness. Woldman et al. [24] also reported that the wear was more if the sharpness of the abrasive particle was high. Researchers revealed that when apex angle of abrasive particles were

lower than the critical value, it can cause high wear. The ineffectiveness beyond the critical value of the apex angle was due to the fact that the abrasive particle gradually becomes round-shaped, and its ability to cause wear decreases. The lower value of the apex angle of the abrasive particle can cause more wear, but it gets easily fractured under the effect of greater load [25-26]. Moreover, few researches carried out investigation to understand the behavior of abrasive particle size on material's wear. In this context, Coronado et al. [27] experimentally proved that the change in wear rate was dependent on the critical size of the abrasive particle. The changes were noticed beyond the CPS (Critical Particle Size), showing the decrease in wear rate responded to an increase in particle size. During two-body sliding abrasion, load changes the ability to cause indentation and cause more surface damage to the material. Furthermore, the effect of load was the primary factor, as wear is directly proportional to the load. Additionally, the manganese steel has the property of work hardenability, that imparts its resistance to wear immensely with increase in load.

The available literature on magnesium steel is in limited amount that didn't delves the effect of abrasive particle size, load, sliding speed, and sliding distance on wear mechanism of magnesium steel. Additionally, the researches conducted on the mechanisms of abrasive wear and the wear resistance of manganese steel, are still deception. Available earlier studies, primarily focused on the said factors in isolation, neglecting their interactive effects which is observed as substantial gaps for this study. Furthermore, while the work-hardening characteristics of manganese steel are well established, its behavior under varying load conditions, particularly in coal-based abrasive settings, has not been thoroughly investigated. Therefore, this study aims to fill that gap by examining the impact of coal particle size on the wear of manganese steel—an aspect that has not been previously addressed in order to create a predictive model. By creating a mathematical model grounded in experimental findings, this research facilitates wear predictions in coal-rich environments, especially for coal bunker liner plates, also offering critical insights for industries that depend on manganese steel components.

2. METHODOLOGY OPTED FOR EXPERIMENTATION

In this experiment, the test specimens, made of manganese steel in the form of pins, were purchased directly from the industry (Maa Bhuneswari Metals, Dhanbad, India). Each pin had a length of 30 mm and a diameter of 12 mm, used for the abrasive wear test, as shown in Figure 1(a). The composition of elements present in the samples was examined through electronic dispersive spectroscopy (EDS) as shown in Figure 1(b).

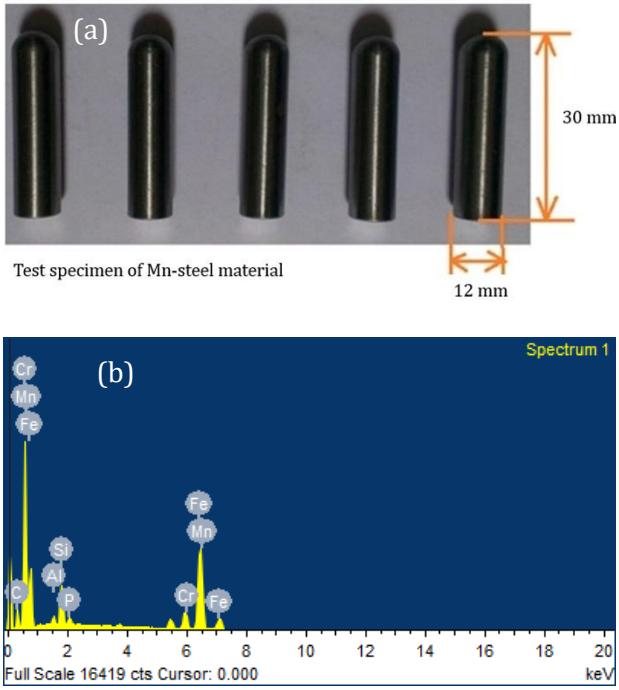

Fig. 1. (a) Images of test specimen samples made from Mn-steel material (b) EDS analysis of manganese steel specimen.

The EDS was taken at five different locations for better analysis. The composition of elements obtained was 14.00 wt. %Mn, 1.35 wt. %C, 1.00 wt. %Si, 0.05 wt. %S and 0.09 wt. %P. Before testing the specimens, metallographic polishing was performed to remove oxide layers and prevent excessive wear at the beginning of the test. This process was also crucial for eliminating all oxides from the surface to ensure optimal results. After polishing, the surface of the specimen was examined under an atomic force microscope to measure the roughness value. The sample roughness was maintained below 0.40 μm for every sample. The wear tests were performed on a pin-on-disc tribometer, and special arrangements were made for coal

particles that act as abrasive material. Since, the author's intention is to develop a predictive model for coal bunker liner plates made of manganese steel to estimate their service life, so, two coal particle sizes, 500 µm and 710 µm, were selected for experimentation. This selection is based on the predominant coal particle sizes found in coal bunker liner plates, typically ranging from 500 to 1000 µm.

The sizes of the coal were separated using a sieve analysis process, with 80% passing through a sieve. Elastic Modulus of abrasive 2.5 GPa, Poisson's ratio 0.34, Hardness of silica content in the abrasive was observed as 982 HV to 991 HV, percentage of silica content in abrasive was found out to be approximately 0.5 to 1.1 percent with varying composition.

2.1 Experimental set-up

A pin-on-disc (DUCOM TR-201LE) wear testing machine, as shown in Figure 2, was used for the two-body abrasive wear process. The machine consists of a rotating plate in the form of a disc, with an attachment to fix the specimens in form of pins. In this study, manganese steel was used for the pin specimens. The wear of the pin specimens was evaluated in relation to the coal particle size placed on the surface of the disc. The disc plate itself had a thickness of 8 mm.

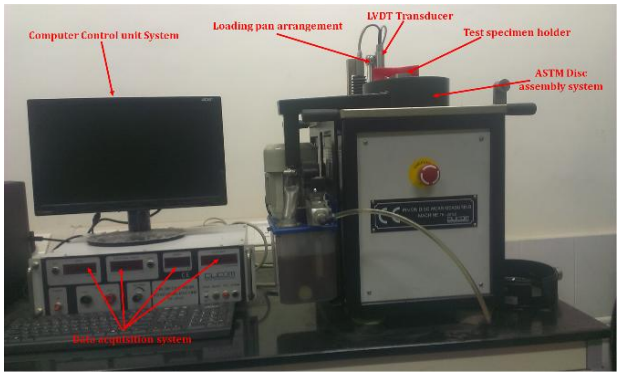

Fig. 2. Pin-on-disc wear measuring machine.

This experimental work followed the ASTM G99-05 (ASTM, 1992) standard. Coal particles were adhered to the surface of the disc plate, as shown in Figure 3. To secure the coal particles to the disc, grooves of 4 mm thick were created extending outward from the center of the disc, as depicted in Figure 4. The remaining surface of the disc was then roughened using a chisel for trapping the coal particles. The coarse surface facilitated the adhesion of the coal particles when adhesive was applied. The coal particles were adhered by properly applying adhesive (like Polyurethane and starch) on the coarse surface of the disc. Once the coal was fully set on the disc, molding was performed, ensuring the coal particles were securely fixed to the disc surface. Two discs were prepared containing uniformly distributed two sizes of coal with bed thickness 4 mm.

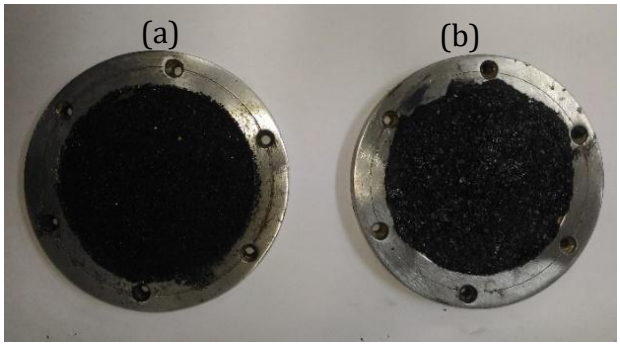

Fig. 3. ASTM G99 standard disc specimen with coal particles of (a) 500 µm and (b) 710 µm.

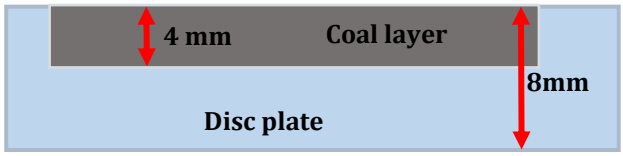

Fig. 4. Layer of coal up to 4 mm fixed on the 8 mm thick disc plate.

After placing the coal particles, the prepared disc plate was heated to 40 ˚C for 15 minutes to eliminate moisture from the coal. The disc was then mounted onto the rotary block of the Pin-on-Disc apparatus. This entire procedure is visually illustrated in Figure 5, offering a clear overview of the process.

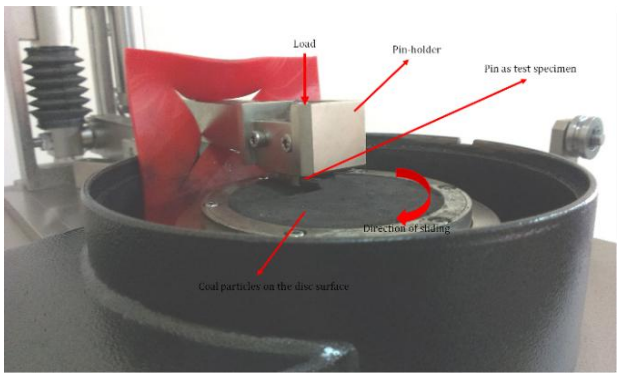

Fig. 5. Image showing the pin is fitted with the test specimen holder and is made to have contact with the disc surface.

Wear tests of manganese steel specimens (pins) were conducted using different plates, each with coal particles of sizes 500 μm and 710 μm. The tests were performed at loads ranging from 20 N to 35 N (specifically 20 N, 25 N, 30 N, and 35 N) in order to observe the material loss in relation to the different coal particle sizes. Weight losses were measured to assess the material's performance against the abrasive action of the particles. The weight loss was recorded in milligrams (mg) using an electronic balance under controlled conditions. Wear tests of each specimen were performed for a fixed sliding distance 1000 m. The surfaces of the pin samples were made flat using emery paper (80-grit size) before each test so that the surfaces remained in full contact with the rotating coal bed surface. The test samples were cleaned with acetone before and after the tests. The samples were immersed in acetone inside a beaker and subjected to sonication to remove all foreign particles from the surface. The specific wear rate was evaluated in terms of mm^3/m-N under different varying conditions using equations 1 & 2.

$$Specific\ wear\ rate\ k = \frac{\Delta V}{P\ X\ L} \quad (1)$$

$$\Delta V = \frac{m_i - m_f}{\delta} \quad (2)$$

Where, k denotes specific wear rate in mm^3/N-m, ΔV denotes change in volume obtained through equation 2. m_i is the initial mass of the specimen, m_f final mass after the test in milligrams, and δ is the mass density. P is the load applied in Newton and L is the sliding distance in meter. Furthermore, the tests were conducted with the disc rotating at a consistent speed of 300 rpm under standard atmospheric conditions (27 °C). A durable EN 31 steel disc (hardness = 60 HRC, HV 695) was chosen as the counter disc for its exceptional strength. It's hardness, nearly ten times that of the experimental sample, ensured a comprehensive evaluation. Notably, the counter disc exhibited no wear during the tests, reflecting the resilience of the materials tested. The investigation repeats three times for each condition, and the average of the same was cited with error.

3. RESULTS AND DISCUSSION ON TRIBOLOGICAL TEST

The effect of load on wear [28-29] is a crucial aspect of tribology and requires thorough investigation to develop a model for prediction. Hence, this experiment first selects four significant loads ranging from low to high. The two abrasive particles of coal adhered to the disc to carry out the experiments. Samples A, B, C, and D are designated as per the load applied on the specimens during the wear test, as shown in Figure 6. For every experiment, the sliding distance was maintained constant in order to make an easy comparison. From Figure 6, a monotonous increase in wear rate was observed with an increase in load up to 30 N for both coal abrasive particles. This happened due to the increased load, the contact pressure between the mating surfaces raises. As a result, there was greater material deformation, leading to higher wear rates. However, interesting features was observed at a higher load of 35 N, i.e., the wear rate improve. The increase in load typically results in higher wear rates due to more significant contact pressure, changes in lubrication conditions, and thermal effects. However, in the case of magnesium steel, the work hardening property predominantly showed its effect and was responsible for the improvement in wear rate. In this regard, Zhang et al. [30] reported that the manganese steels had good work hardening properties. This allows the material to resist wear with an increase in sliding abrasion. At higher loads, deep grooves and surface cavities formed that result in acceleration of wear rate. When the load is very high, there is a possibility that abrasive coal particles may become embedded in the specimen's surface, preventing direct contact between the mating surfaces. This can lead to reduced material loss, resulting in a decrease in the wear rate [31-32]. Additionally, the surface hardening property with normal load may prevent loss of material from the surface and result in decrement of wear rate. Higher loads improve interfacial bond-bearing capacity between the specimen and the particles, which reduces the possibility of surface material to get pulled out [33]. Also, the subsurface of the test specimen under higher load develops a work-hardening property for which cutting ability by the abrasive particle decreases.

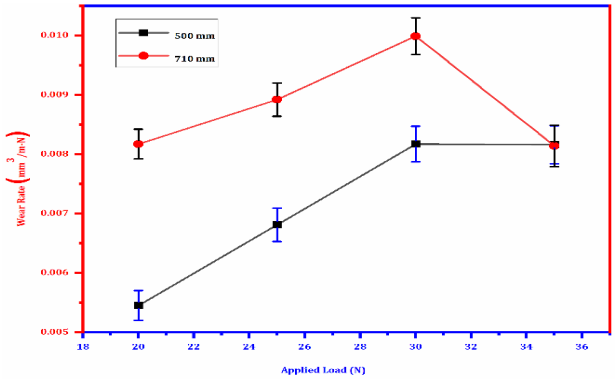

Fig. 6. Plots of weight loss of test specimen with variation of load 500 µm and 710 µm.

Furthermore, larger grains can reduce the overall toughness of a material. This makes it more susceptible to cracking and chipping under load, which can contribute to wear. So, higher grain sizes effectively produce a high worn-out surface of material up to a particular load. However, at a very high load, due to the predominance of the work hardening property, the wear rate significantly decreases. A similar mechanism was earlier revealed by Petrica et al. [34] that the manganese steel material showed a transition in wear mechanism due to which the surface property during abrasion changes, which leads to minimum wear at high load. The SEM and EDS images of Pin before and after the test are shown in Figure 7 and 8.

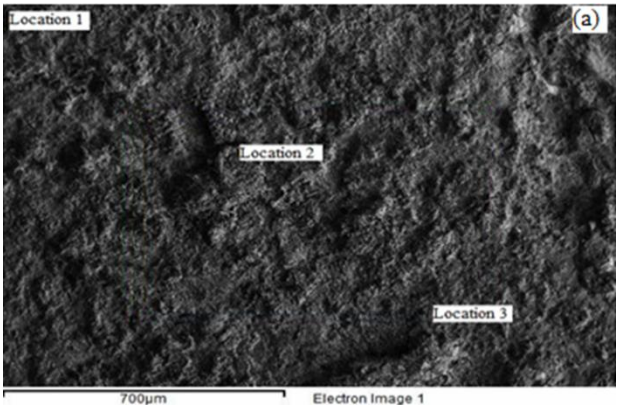

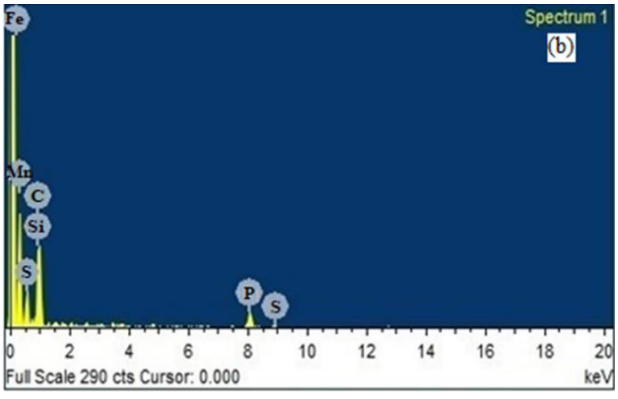

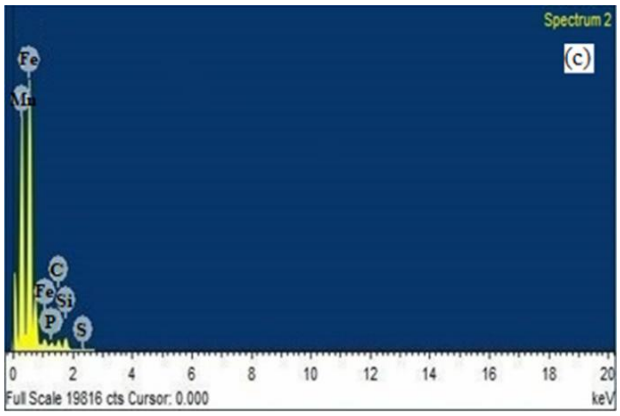

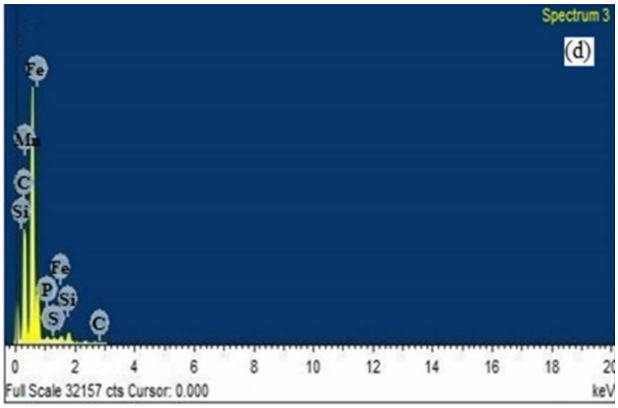

Fig. 7. SEM and EDS images of Pin before test.

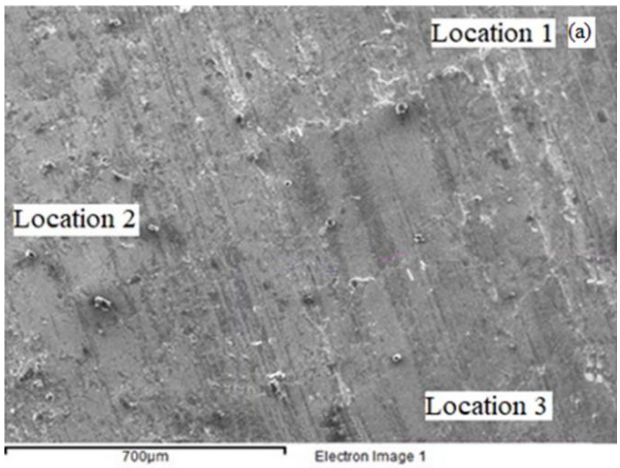

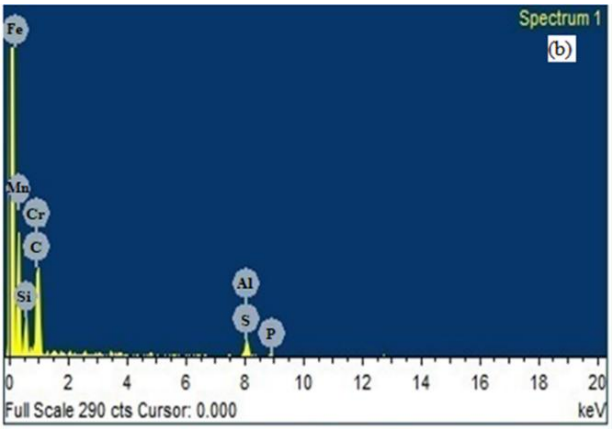

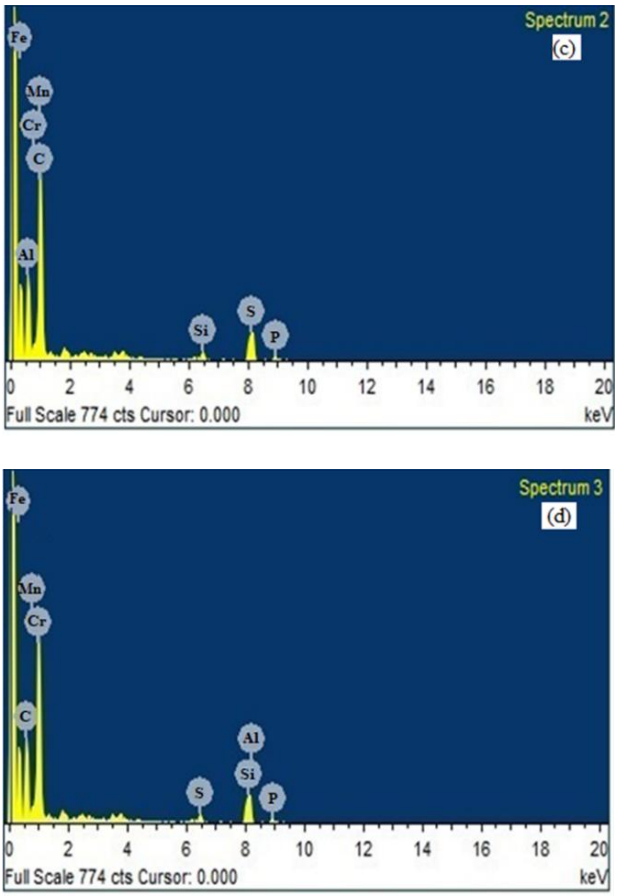

Fig. 8. SEM and EDS images of Pin after test.

3.1 Discussion based on SEM images

From the experiments, it was observed that the weight loss of the specimen increases with increasing load from 20 N to 30 N. However, at a high load around 35N, a significant improvement in wear rate was observed. The coal particle having a 710 μm size causes more wear than 500 μm at medium to normal load. However, at high loads, the work-hardening ability of manganese steel also improved with wear rate to some extent. So, in this section, a discussion is made with SEM images of the worn surfaces in order to identify the type of surface damage that occurred. SEM microphotographs obtained for the specimens worn out due to sliding on coal particle size for 500 μm are presented in Figure 9(a-d). In comparison, Figure 10(a-d) shows the surface damage of the worn-out specimen while testing through a coal particle size of 710 μm. The images show that the damages were created in the form of scratches and grooves responsible for severely damaging the surface of the specimen. From Figure 9(a), it is clearly observed that the worn track or scratches formed were smoother and lighter compared to all other SEM images.

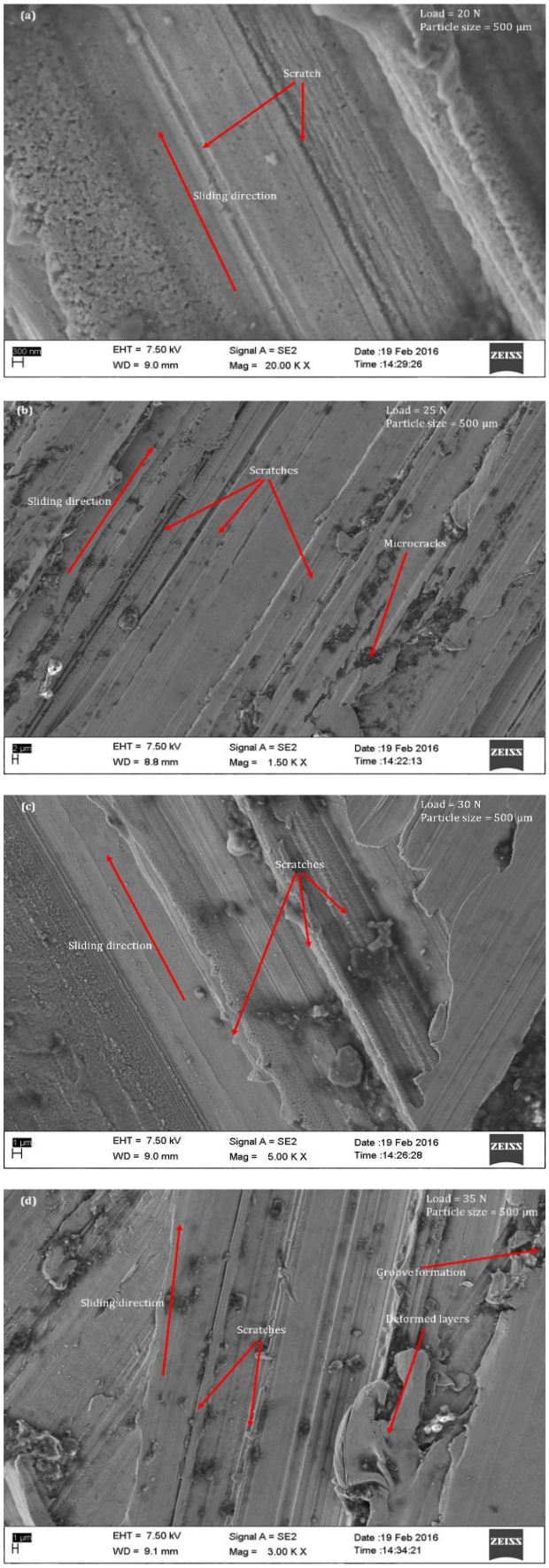

Fig. 9. Microscopy images of damaged surface of pin specimen under SEM when specimen slides on coal particle size of 500 μm.

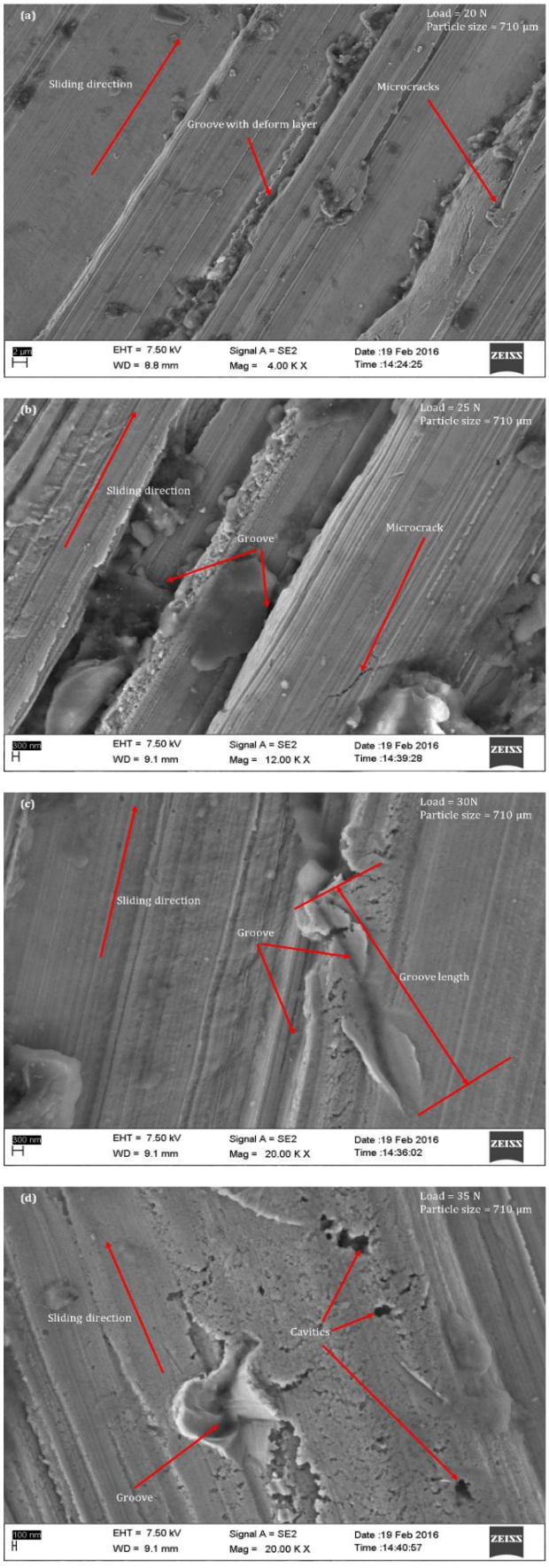

Fig. 10. Microscopy images of damaged surface pin specimen under SEM when specimen slides on coal particle size of 710 µm.

Meanwhile, for other images, higher scratches with more prominent grooves formed. This happened due to the high load acting on the contacting body, led to high Hertzian pressure, consequence to increase in the contact area of abrasive particles during sliding [35]. However, at a very high load, some improvement was noticed due to the work-hardening effect. Similar findings were also observed from the SEM images of 710-micron coal particles. The formation of scratches or grooves were large with increase in load. Hence, the microphotographs reveal that with the increase in load, there was a transition in wear mechanisms. The transition was observed from scratch to groove formation. However, some marks of cavities were also observed at high loads. Large-size coal particles produce more damage than small-size particles. Also, from the obtained microphotographs, there was some evidence of microcrack formation at low load. This shows that at higher loads, new surface layers were developed, results in fresh development of surface damage.

3.2 Theoretical approach to measure material losses

The abrasivity of the particle increases with the presence of hard elements. Silica is considered a hard mineral whose presence increases the hardness of abrasive particles. Mostly, abrasive particles have a sharp edge, which increases their ability to penetrate inside the bulk material to high degree. The sharp edge of the abrasive particle is determined by the apex angle [36-37]; with the decrease in apex angle, sharpness of grain increases. But there is a critical value up to which the sharpness of abrasive particles causes wear reported by Hamlin and Stachowiak [38]. In studies researchers used the term spike value to define the sharpness of abrasive particles and strive to evaluate the effect of apex angel on wear rate. The spike value was the product of half of the apex angle and triangle height, which was made by fitting the line at the sharp edges as shown in Figure 11. Researchers also noticed that as the size of abrasive particles increases, wear was more. This was attributed to the increase in the spike value of the abrasive particle. Also, a small value of the apex angle gets fractured easily under the effect of high load, observed in some cases. The grains used to measure the apex angle for calculation of material sizes are shown in

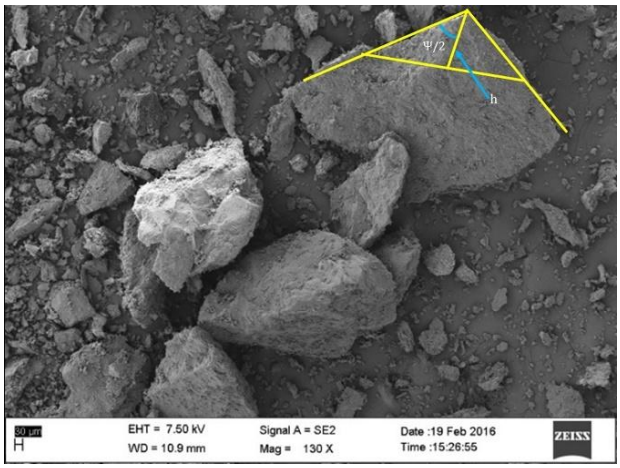

Fig. 11. Pictorial image under SEM showing abrasivity of particle in terms of apex angle (ψ).

Figure 12 (a) and (b). The average of apex angles was considered to develop the predictive model in order to calculate the material loss due to formation of groove.

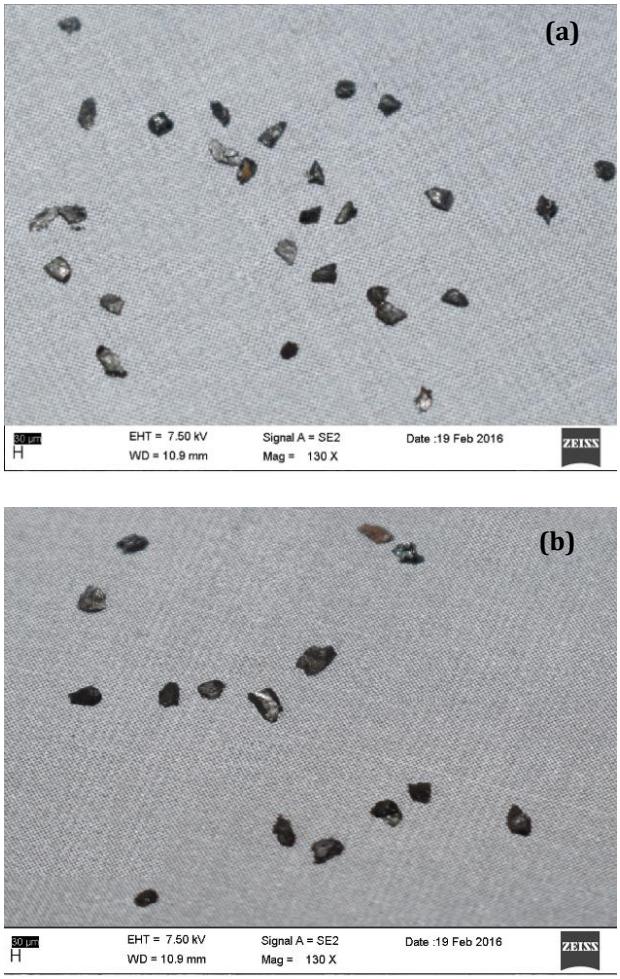

Fig. 12. (a) Number of 500 µm particles used to measure apex angle (b) Number of 710 µm particles measure apex angle.

When an abrasive particle slides on the material surface, it produces grooves on the surface of the material. The formed groove on the material surface depends on the apex angle of the abrasive particle. To theoretically calculate the amount of material losses from the formed groove, it is assumed that the abrasive particle, when it slides on the surface of the material, produces a uniform depth of groove for the length of 'x'. This is shown in Figure 13.

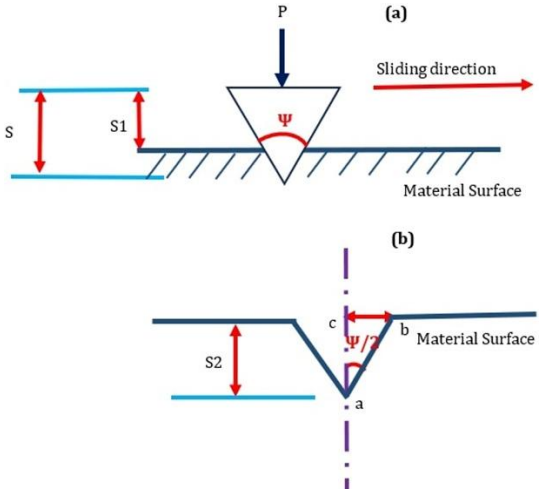

Fig. 13. (a) Abrasive particle in contact with the material surface, (b) Groove of height S_2 on the material surface

In Figure 13(a), initially, load 'P' is applied on the abrasive particle of size 'S' and apex angle 'ψ' to indent on the material surface. An abrasive particle then produces a groove of depth 'S2'; the depth 'S_2' is also the indentation depth of the abrasive particle. Assuming that the groove formed during indentation is a triangle in shape. This is shown in Figure 13(b). As the abrasive particle slides a distance of the 'x' unit, it produces a groove of length 'x.' According to Archard et al. [39], the stiffness 'S' material was defined as the resistance of the material to resist deformation. In the indentation process, it is the ratio of load (P) to the displacement made (S_2) on the surface during penetration. It is written as

$$S = \frac{P}{s_2} \tag{3}$$

$$S = 2E^*\beta\sqrt{\frac{A}{\pi}} \tag{4}$$

$$\text{And} \quad E^* = \left[\left(\frac{1-\nu^2}{E}\right) + \left(\frac{1-\nu_i^2}{E_i}\right)\right]^{-1} \tag{5}$$

Where, S is the stiffness, E* is the reduced modulus, and A is the contact area of the sharp edge of an abrasive particle with the material surface. β is the constant parameter of the sharp edge of the particle. For a triangular shape, the value of β is 1.034. The groove is assumed to be a triangle in shape. The area of the triangle can be calculated as

$$A = \frac{s_2.r}{2} \tag{6}$$

Where, r is half of the radius of the triangle.

From Figure 13(b), the depth s_2 is calculated as

$$ab = \frac{s_2}{sin(\psi/2)} \tag{7}$$

$$\text{And} \quad s_2 = \sqrt{(ab)^2 - r^2} \tag{8}$$

$$\text{Or} \quad s_2 = r\sqrt{\frac{1-sin(\psi/2)}{sin(\psi/2)}} \tag{9}$$

Therefore, the area of triangle is written as

$$A = \frac{r^2}{2}\sqrt{\frac{\{1-sin(\psi/2)\}^2}{\{sin(\psi/2)\}^2}} \tag{10}$$

Assuming abrasive particle slides for a distance of 'x' unit, thus forming a groove of length 'x' unit. Considering the volume of material loss, V, to be proportional to the area and sliding distance, then we have

$$V \propto A.x \tag{11}$$

$$V = k.A.x \tag{12}$$

Where, k is the proportionality constant, which is the wear coefficient subsequently,

$$V = \left(\frac{k.s_2.r}{2}\right).x \tag{13}$$

$$\text{Or} \quad V = \left(\frac{k.P.r}{2S}\right)x \tag{14}$$

Substituting Equation 2 in Equation 14,

$$V = \left(\frac{k.P.r}{4E^*\beta\sqrt{\frac{A}{\pi}}}\right).x \tag{15}$$

Substituting Equation 8 in Equation 15,

$$V = \left(\frac{\sqrt{\pi}}{2.82\beta}\right)\left(\frac{k.P.x}{E^*}\right)\frac{1}{1/4\sqrt{\frac{\{1-sin(\psi/2)\}^2}{(sin(\psi/2))^2}}} \tag{16}$$

The above equation is the simplest form of the equation, which gives an approximate amount of material removed from the groove. The unit of volume loss is in 'mm^3'. Equation 16 is the function of load, sliding distance, and reduced elastic modulus of both the contacting bodies.

Geometric constant β represents the shape of particles. Its value is 1.034 for conical-shaped particles [38]. The value of kin wear models varies from 10^{-4} to 10^{-1}. In this study, the value of k is selected as 10^{-1}, which is the value of the coefficient of friction between coal and the manganese steel liner plate.

3.3 Validation with experimental results

The apex angle of the coal particles was measured using the Image analysis technique. The apex angle of coal was observed to be in the range between 12.703° to 29.321°. The cumulative value of the apex angle was taken as 25.169°. The elastic modulus and Poisson's ratio of coal were considered as 1.641 GPa and 0.35, respectively. Meanwhile, for manganese steel, the value of elastic modulus is taken as 187 GPa, Poission's ratio is 0.23, and the density of manganese steel is 7.35 g/cm^3. Then, the reduced modulus is calculated as 1.83822 GPa. The predicted volume loss with respect to the obtained weight loss is presented in Figure 14.

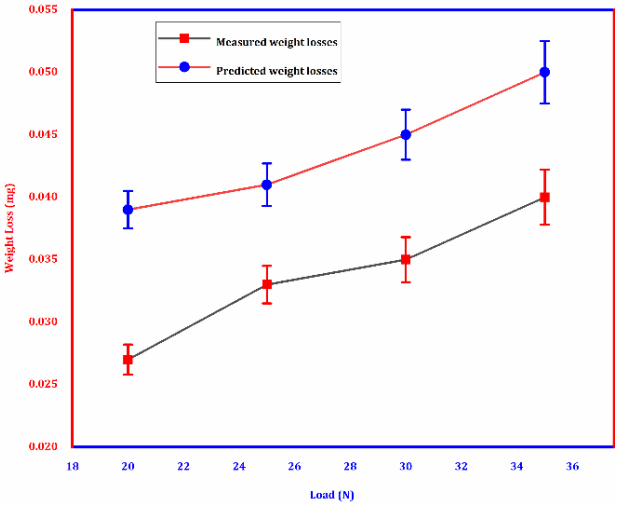

Fig. 14. Measured and predicted weight loss

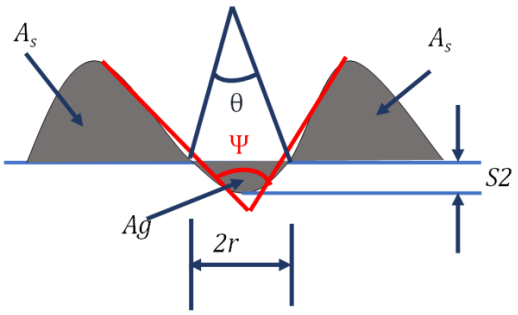

Fig. 15. Deformed layers near to the side of the groove of width 2r and height S_2 with area of A_g.

The result complied in Figure 14 shows significant deviation in weight loss from evaluated value to predicted value. This is probably due to the approximate calculation of weight losses from Equation 16. Additionally, in wear operations, the formation of grooves is frequently accompanied by the development of deformed layers, as illustrated in Figure 15. These deformed layers arise from plastic deformation, the displacement of material, and the accumulation of residual stress at the edges of the grooves. The existence of these layers has a significant impact on overall material removal efficiency, surface quality, and the mechanical characteristics of the finished component. Then, for the deformed layers, the total volume removed can be calculated as follows [40]:

The total volume of material removed is $V_g - V_s$. Where, V_g is the volume removed from the groove, and V_s is the volume of deformed layers at the side of the groove.

Additionally, the result contradicts the cited predicted model developed by Rabinowicz wear model [21], in which the error level was much higher. The predictive values from the extended equation were controlled under 36%. The error level was high but paved a way to develop the futuristic investigation in order to get highly efficient model. The erratic error levels between the measured values and predictive values were affected because of the frequent dismantling of test specimens, shocks and measurement error that need to encounter during the experimental process. The accuracy rate can be improved if experiments are carried out in a more controlled environment. Also, there remains a range of other key variables like fracture toughness of the alloys and porosity of coal that may require to be included in the extended model to reduce the percentage of error within an acceptable limit.

4. CONCLUSIONS

This investigation successfully showed the effect of load (20-35 N) and coal particles (i.e., 500 μm and 710 μm as abrasive material) on the wear rate of manganese steel. From the results of abrasive wear experiments, it has been noted that with an increase in load, the wear of manganese steel monotonically increases up to a specific limit. The research also reveals that larger coal particles cause more damage to the material surface than smaller coal particles. However, interesting results were obtained at higher loads, and the wear rate improved significantly. The improvement is attributed to the peculiar advantages of properties governed by manganese steel, i.e., work hardening. It is also noted from the SEM microphotographs that small particles create scratch-type surface damage. In comparison, the large size of particles creates high surface damage in the form of grooves. The length of the groove decreases with an increase in load. At a load of 35 N, the depth of penetration was higher than that of the long-length groove obtained at 30 N of load. There was a transition in the wear mechanism with the change in load due to the work-hardening property of the material, as coal particles produce more scratches and grooves on the material surface. Furthermore, a theoretical approach has been made to calculate the volume of material loss from the formed grooves. This theoretical approach will help to understand the effective parameters that are influencing the material losses in two-body abrasive wear conditions. The approach to calculating material loss volume from formed grooves in wear analysis should correctly consider all assumption of idealized groove geometry. Further, the real-world wear mechanisms involve complex deformation, material displacement, and irregular groove shapes that are difficult to accurately model mathematically, which need to take care during assumption processes. Additionally, factors such as strain hardening, microstructural variations, and secondary wear mechanisms (e.g., oxidation and fatigue) are often not fully accounted for, leading to deviations between theoretical predictions and actual wear behavior.

Acknowledgement

The authors thank the management and staff of Elitte college of Engineering for their incessant help.

REFERENCES

[1] H. P. Jost, "Tribology — Origin and future," *Wear*, vol. 136, no. 1, pp. 1–17, Feb. 1990, doi: 10.1016/0043-1648(90)90068-l.

[2] A. Davies, *Handbook of Condition Monitoring*. 1998. doi: 10.1007/978-94-011-4924-2.

[3] A. Misra and I. Finnie, "Some observations on two-body abrasive wear," *Wear*, vol. 68, no. 1, pp. 41–56, Apr. 1981, doi: 10.1016/0043-1648(81)90018-1.

[4] N. C. Sinha, B. K. Sinha, T. K. Roy, and S. R. Krishnan, "Abrasion characteristics of coals," *Fuel*, vol. 61, no. 12, pp. 1285–1286, Dec. 1982, doi: 10.1016/0016-2361(82)90037-0.

[5] B. K. Singh, A. Kumar, R. Cep, A. Kumar, A. Kumar, N. Dogra, and K. Logesh, "Behavior of CuO as solid lubricant inside ZTA matrices," *AIP Advances*, vol. 14, no. 8, Aug. 2024, doi: 10.1063/5.0213553.

[6] A. Dumay, J. -p. Chateau, S. Allain, S. Migot, and O. Bouaziz, "Influence of addition elements on the stacking-fault energy and mechanical properties of an austenitic Fe–Mn–C steel," *Materials Science and Engineering A*, vol. 483–484, pp. 184–187, May 2007, doi: 10.1016/j.msea.2006.12.170.

[7] S. F. Scieszka, "A technique to study abrasive wear in contacts with particulate materials," *Wear*, vol. 119, no. 2, pp. 237–249, Sep. 1987, doi: 10.1016/0043-1648(87)90113-x.

[8] Q. Luo and J. Zhu, "Wear property and wear mechanisms of High-Manganese austenitic hadfield steel in dry reciprocal sliding," *Lubricants*, vol. 10, no. 3, p. 37, Mar. 2022, doi: 10.3390/lubricants10030037.

[9] Y. H. Wen, H. B. Peng, H. T. Si, R. L. Xiong, and D. Raabe, "A novel high manganese austenitic steel with higher work hardening capacity and much lower impact deformation than Hadfield manganese steel," *Materials & Design (1980-2015)*, vol. 55, pp. 798–804, Oct. 2013, doi: 10.1016/j.matdes.2013.09.057.

[10] G. Tressia, J. J. Penagos, and A. Sinatora, "Effect of abrasive particle size on slurry abrasion resistance of austenitic and martensitic steels," *Wear*, vol. 376–377, pp. 63–69, Apr. 2017, doi: 10.1016/j.wear.2017.01.073.

[11] W. Yan, L. Fang, K. Sun, and Y. Xu, "Effect of surface work hardening on wear behavior of Hadfield steel," *Materials Science and Engineering A*, vol. 460–461, pp. 542–549, Mar. 2007, doi: 10.1016/j.msea.2007.02.094.

[12] J. Kang, F. C. Zhang, X. Y. Long, and B. Lv, "Cyclic deformation and fatigue behaviors of Hadfield manganese steel," *Materials Science and Engineering A*, vol. 591, pp. 59–68, Oct. 2013, doi: 10.1016/j.msea.2013.10.072.

[13] S. Sathish, V. Anandakrishnan, and M. Gupta, "Optimization of tribological behavior of magnesium metal-metal composite using pattern search and simulated annealing techniques," *Materials Today Proceedings*, vol. 21, pp. 492–496, Jul. 2019, doi: 10.1016/j.matpr.2019.06.643.

[14] O. A. Zambrano, Y. Aguilar, J. Valdés, S. A. Rodríguez, and J. J. Coronado, "Effect of normal load on abrasive wear resistance and wear micromechanisms in FeMnAlC alloy and other austenitic steels," *Wear*, vol. 348–349, pp. 61–68, Dec. 2015, doi: 10.1016/j.wear.2015.11.019.

[15] E. Bayraktar, F. A. Khalid, and C. Levaillant, "Deformation and fracture behaviour of high manganese austenitic steel," *Journal of Materials Processing Technology*, vol. 147, no. 2, pp. 145–154, Mar. 2004, doi: 10.1016/j.jmatprotec.2003.10.007.

[16] W. Song, T. Ingendahl, and W. Bleck, "Control of strain hardening behavior in High-MN austenitic steels," *Acta Metallurgica Sinica (English Letters)*, vol. 27, no. 3, pp. 546–556, Jun. 2014, doi: 10.1007/s40195-014-0084-9.

[17] D. T. Pierce, J. A. Jiménez, J. Bentley, D. Raabe, and J. E. Wittig, "The influence of stacking fault energy on the microstructural and strain-hardening evolution of Fe–Mn–Al–Si steels during tensile deformation," *Acta Materialia*, vol. 100, pp. 178–190, Aug. 2015, doi: 10.1016/j.actamat.2015.08.030.

[18] O. Acselrad, A. R. De Souza, I. S. Kalashnikov, and S. S. Camargo, "A first evaluation of the abrasive wear of an austenitic FeMnAlC steel," *Wear*, vol. 257, no. 9–10, pp. 999–1005, Aug. 2004, doi: 10.1016/j.wear.2004.07.004.

[19] S. Mahdavi and F. Akhlaghi, "Effect of the SiC particle size on the dry sliding wear behavior of SiC and SiC–Gr-reinforced Al6061 composites," *Journal of Materials Science*, vol. 46, no. 24, pp. 7883–7894, Jul. 2011, doi: 10.1007/s10853-011-5776-1.

[20] R. Sinha and A. K. Mukhopadhyay, "Wear characterization and modelling of Mn–steel liners used in rock crushers," *Perspectives in Science*, vol. 8, pp. 374–376, May 2016, doi: 10.1016/j.pisc.2016.04.079.

[21] E. Rabinowicz and A. Mutis, "Effect of abrasive particle size on wear," *Wear*, vol. 8, no. 5, pp. 381–390, Sep. 1965, doi: 10.1016/0043-1648(65)90169-9.

[22] A. G. Wang and I. M. Hutchings, "The number of particle contacts in two-body abrasive wear of metals by coated abrasive papers," *Wear*, vol. 129, no. 1, pp. 23–35, Jan. 1989, doi: 10.1016/0043-1648(89)90276-7.

[23] M. A. Moore and R. M. Douthwaite, "Plastic deformation below worn surfaces," *Metallurgical Transactions A*, vol. 7, no. 12, pp. 1833–1839, Dec. 1976, doi: 10.1007/bf02659813.

[24] M. Woldman, E. Van Der Heide, T. Tinga, and M. A. Masen, "The influence of abrasive body dimensions on single asperity wear," *Wear*, vol. 301, no. 1–2, pp. 76–81, Dec. 2012, doi: 10.1016/j.wear.2012.12.009.

[25] G. Srinath and R. Gnanamoorthy, "Two-body abrasive wear characteristics of Nylon clay nanocomposites—effect of grit size, load, and sliding velocity," *Materials Science and Engineering A*, vol. 435–436, pp. 181–186, Sep. 2006, doi: 10.1016/j.msea.2006.07.117.

[26] Thakare, J. A. Wharton, R. J. K. Wood, and C. Menger, "Effect of abrasive particle size and the influence of microstructure on the wear mechanisms in wear-resistant materials," *Wear*, vol. 276–277, pp. 16–28, Dec. 2011, doi: 10.1016/j.wear.2011.11.008.

[27] J. J. Coronado, S. A. Rodríguez, and A. Sinatora, "Effect of particle hardness on mild–severe wear transition of hard second phase materials," *Wear*, vol. 301, no. 1–2, pp. 82–88, Dec. 2012, doi: 10.1016/j.wear.2012.12.016.

[28] B. K. Singh, "State-of-Art on Self-Lubricating Ceramics and Application of CU/CUO as solid lubricant material," *Transactions of the Indian Ceramic Society*, vol. 82, no. 1, pp. 1–13, Jan. 2023, doi: 10.1080/0371750x.2022.2149625.

[29] K. Raja, P. Ganeshan, B. K. Singh, R. K. Upadhyay, P. Ramshankar, and V. Mohanavel, "Effect of mol.% of Yttria in Zirconia matrix alongside a comparative study among YSZ, alumina & ZTA ceramics in terms of mechanical and functional properties," *Sadhana*, vol. 48, no. 2, Apr. 2023, doi: 10.1007/s12046-023-02136-w.

[30] Z. F. Zhang, L. C. Zhang, and Y. -w. Mai, "Particle effects on friction and wear of aluminium matrix composites," *Journal of Materials Science*, vol. 30, no. 23, pp. 5999–6004, Dec. 1995, doi: 10.1007/bf01151519.

[31] S. K. Gautam, B. K. Singh, R. K. Singh, S. K. Tiwari, R. Upadhyaya, H. Khandelwal, G. Kumar, S. M. M. Hasnain, and R. Zairov, "Advancements in Semi-Solid Metal Processing of ADC12 Aluminium Alloy: Microstructure and Mechanical Properties," *Results in Engineering*, p. 104453, Feb. 2025, doi: 10.1016/j.rineng.2025.104453.

[32] W. Grzegorzek, D. Adamecki, G. Głuszek, A. Lutyński, and D. Kowol, "Technique to investigate pulverizing and abrasive performance of coals in mineral processing systems," *Energies*, vol. 14, no. 21, p. 7300, Nov. 2021, doi: 10.3390/en14217300.

[33] B. K. Singh, S. K. Gautam, A. Anand, R. K. Singh, S. K. Tiwari, A. R. Subhani, and R. Upadhyaya, "Parametric study to investigate mechanical properties of welded dissimilar Al6063 and Al 7073 alloys through FSW process," *Engineering Research Express*, vol. 6, no. 3, p. 035406, Jul. 2024, doi: 10.1088/2631-8695/ad5f79.

[34] M. Petrica, E. Badisch, and T. Peinsitt, "Abrasive wear mechanisms and their relation to rock properties," *Wear*, vol. 308, no. 1–2, pp. 86–94, Oct. 2013, doi: 10.1016/j.wear.2013.10.005.

[35] D. O. Moumakwa and K. Marcus, "Tribology in coal-fired power plants," *Tribology International*, vol. 38, no. 9, pp. 805–811, Apr. 2005, doi: 10.1016/j.triboint.2005.02.009.

[36] A. K. Srivastava, P. Pal, A. Pal, B. K. Singh, R. Kumar, and A. Kumar, "Parametric evaluation & optimization of wire-EDM process for machining of super alloy materials (EN-24 steel) in terms of surface integrity and material removal rate," *AIP Conference Proceedings*, vol. 3232, p. 020033, Jan. 2024, doi: 10.1063/5.0235844.

[37] M. G. Hamblin and G. W. Stachowiak, "A multi-scale measure of particle abrasivity," *Wear*, vol. 185, no. 1–2, pp. 225–233, Jun. 1995, doi: 10.1016/0043-1648(95)06624-1.

[38] M. G. Hamblin and G. W. Stachowiak, "A multi-scale measure of particle abrasivity, and its relation to two-body abrasive wear," *Wear*, vol. 190, no. 2, pp. 190–196, Dec. 1995, doi: 10.1016/0043-1648(95)06677-2.

[39] J. F. Archard, "Elastic deformation and the laws of friction," *Proceedings of the Royal Society of London a Mathematical and Physical Sciences*, vol. 243, no. 1233, pp. 190–205, Dec. 1957, doi: 10.1098/rspa.1957.0214.

[40] E. Rabinowicz, "Friction and wear of Self-Lubricating metallic materials," *Journal of Lubrication Technology*, vol. 97, no. 2, pp. 217–220, Apr. 1975, doi: 10.1115/1.3452560.